

The Lasting Effects of Low-Frequency Repetitive Transcranial Magnetic Stimulation on Resting State EEG in Healthy Subjects

Shuang Qiu¹, Weibo Yi, Shengpei Wang, Chuncheng Zhang, and Huiguang He

Abstract—Repetitive transcranial magnetic stimulation (rTMS) is a noninvasive brain stimulation technique that can influence cortical excitability. Low-frequency rTMS (stimulation frequency ≤ 1 Hz) can induce inhibitory effects on cortical excitability. In order to investigate dynamic changes in neuronal activity after low-frequency rTMS, 20 healthy subjects received 1-Hz rTMS over the right motor area, and electroencephalography (EEG) in resting condition with eyes open was recorded before rTMS and at 0 min, 20 min, 40 min, and 60 min after rTMS. Power values, functional connectivity based on a weighted phase lag index (wPLI), and network characteristics were assessed and compared to study the aftereffects of rTMS. Our results show that low-frequency rTMS produced a delayed long-lasting increase in alpha-band power values in frontoparietal brain areas and an immediate long-lasting increase in theta-band power values in the ipsilateral frontal and contralateral centroparietal areas. In the alpha band, functional connectivity decreased immediately after rTMS but significantly increased at 20 min after rTMS. Moreover, an analysis of undirected graphs revealed that the number of connections significantly changed in the anterior and posterior regions in the alpha band. In addition, there were significant decreases in clustering coefficients of the channels near the site of stimulation in the alpha and

theta bands after rTMS. In conclusion, low-frequency rTMS produces widespread and long-lasting alterations in neural oscillation and functional connectivity. This work implies that low-frequency rTMS can induce inhibitory effects on motor cortical excitability ipsilateral to the stimulation site.

Index Terms—Repetitive transcranial magnetic stimulation, low-frequency, resting state EEG, power, functional connectivity.

I. INTRODUCTION

TRANSCRANIAL magnetic stimulation (TMS) is a noninvasive brain stimulation method that applies magnetic pulses to produce targeted alterations of cortical physiologic functions [1]–[4]. Repetitive TMS (rTMS) that TMS pulses are delivered repetitively, can influence cortical excitability [5], [6]. Generally, excitability is inhibited if the stimulation frequency is 1 Hz or less, which is called “low-frequency rTMS”, whereas “high-frequency rTMS” with a frequency of 5 Hz or more usually leads to an increase in cortical excitability [7], [8]. Moreover, the effects of rTMS in cortical activity can persist and influence motor and cognitive functions long beyond the duration of the TMS train itself [9]–[13]. So far, the majority of studies applied low-frequency rTMS over the unaffected hemisphere to promote functional recovery after stroke [14], [15], which leads to positive effects on motor recovery in patients with stroke [16], [17]. Such aftereffects are at the heart of the rTMS protocols in cognitive neuroscience and neurotherapeutics [11]. On the one hand, the applications of rTMS depend on the magnitude and duration of these aftereffects. On the other hand, the investigations of the aftereffects are very helpful to understand the mechanisms of rTMS. Therefore, there is great interest in the investigations of lasting effects after rTMS for the therapeutic applications of rTMS.

Electroencephalography (EEG) is a more sensitive and direct measure for evaluating effects of rTMS on brain functions than behavioral data [11]. Recent developments that combine TMS with EEG have extended the investigation of the modulation of cortical excitability [18]–[21]. These studies are derived from the measurement of evoked potentials (EPs) after single-pulse TMS to study brain states. TMS-evoked potentials offer a powerful tool for measuring causal interactions in the human brain, since the source of stimulation is known and can be experimentally controlled [22]. Recently, in order to estimate the effect of rTMS on brain functions, neural oscillations before and after rTMS have been measured and

Manuscript received November 1, 2019; revised January 6, 2020 and February 17, 2020; accepted February 25, 2020. Date of publication March 3, 2020; date of current version April 8, 2020. This work was supported in part by the National Natural Science Foundation of China under Grant 81701785, Grant 61976209, and Grant 61906188, in part by the Strategic Priority Research Program of Chinese Academy of Sciences (CAS) under Grant XDB32040000, and in part by the China Postdoctoral Science Foundation under Grant 2019M650893. (Shuang Qiu and Weibo Yi contributed equally to this work.) (Corresponding authors: Shuang Qiu; Huiguang He.)

Shuang Qiu and Chuncheng Zhang are with the Research Center for Brain-Inspired Intelligence, Institute of Automation, Chinese Academy of Sciences, Beijing 100190, China (e-mail: shuang.qiu@ia.ac.cn; chuncheng.zhang@ia.ac.cn).

Weibo Yi is with the Beijing Machine and Equipment Institute, Beijing 100854, China (e-mail: yiweibo1987@163.com).

Shengpei Wang is with the School of Artificial Intelligence, University of Chinese Academy of Sciences, Beijing 100049, China, and also with the Research Center for Brain-Inspired Intelligence, Institute of Automation, Chinese Academy of Sciences, Beijing 100190, China (e-mail: wangshengpei2014@ia.ac.cn).

Huiguang He is with the Research Center for Brain-Inspired Intelligence, National Laboratory of Pattern Recognition, Institute of Automation, Chinese Academy of Sciences, Beijing 100190, China, also with the School of Artificial Intelligence, University of Chinese Academy of Sciences, Beijing 100049, China, and also with the Center for Excellence in Brain Science and Intelligence Technology, Chinese Academy of Sciences, Beijing 100864, China (e-mail: huiguang.he@ia.ac.cn).

This article has supplementary downloadable material available at <http://ieeexplore.ieee.org>, provided by the authors.

Digital Object Identifier 10.1109/TNSRE.2020.2977883



Fig. 1. Experimental paradigm.

compared [23]. Griskova and colleagues reported an overall increase in delta power induced by 10 Hz rTMS over the left dorsolateral prefrontal cortex [24]. Fuggetta *et al.* found that high-frequency rTMS over the motor cortex affected oscillatory activity in the alpha and beta bands [25]. Also, EEG theta-band oscillations were increased and alpha-band oscillations were decreased by the 5Hz rTMS over the superior parietal lobe [26].

More recently, several studies have used EEG to investigate the modulation on functional connectivity induced by rTMS. In 2014, a combined TMS-EEG study found that continuous theta-burst rTMS over the motor cortex decreased functional connectivity in the alpha and high-beta band of resting state EEG [10]. Another recent study reported that the functional connectivity and network characteristics of regions related to motor functions could be significantly changed by low-frequency rTMS over the non-dominant motor cortex as well as through motor training [20]. All these findings show that oscillatory activity and functional connectivity of resting state EEG are effective methods to explore aftereffects induced by rTMS.

Previous studies have demonstrated that aftereffects on evoked potentials can last up to 70min after one session of conventional rTMS [11]. This observed aftereffect duration is comparable with the TMS-induced aftereffects on corticospinal motor excitability measured via EMG. To study on changes in oscillatory activity and functional connectivity induced by rTMS, the majority of studies compared EEG activity before and after rTMS to investigate the effect of rTMS on cortical functions. However, data on neural oscillatory and functional connectivity collected during one experimental session after rTMS do not provide sufficient information to assess dynamic changes after rTMS. Thus, in order to understand the modulation on cortical functions induced by rTMS, it is critical to analyze the dynamic changes in EEG that can be observed after rTMS. Few studies have investigated dynamic changes in neural oscillatory or functional connectivity after rTMS by measuring EEG across several sessions after rTMS. Stren *et al.* found that 1 Hz rTMS causes a persistent increase in the alpha-band coherence between C3-CP3 and F3-FC3, immediately following rTMS and at 25 min after low-frequency rTMS. However, Shafi *et al.* measured 30min resting state EEG after low-frequency rTMS and found a widespread decrease in functional connectivity in the alpha band. The inconsistency between these two studies may be due to different experiment setups and the different analysis techniques. Hence, the dynamic changes in functional connectivity after rTMS are still unclear. Moreover, in 2018, Desideri *et al.* applied alpha-rhythm phase-dependent burst-rTMS over the left motor cortex to investigate the effect of rTMS on cortical excitability from resting state EEG, comparing between two sessions before rTMS and three sessions after rTMS [27]. The authors did not observe significant changes

in any EEG response they measured. One explanation for this null finding might be that they just analyzed alpha and beta powers in C3 and C4 channels, rather than power changes across a number of EEG channels. Although several previous studies have analyzed power and functional connectivity at different time after rTMS, the dynamic changes in EEG activity after rTMS have not been reliably determined. Therefore, it is necessary to measure EEG activity from more channels, during multi-sessions, and at longer durations.

The present study aimed to explore aftereffects of rTMS through analyzing EEG activity in a high number of channels up to 70min after rTMS. For motor function rehabilitation of patients with stroke, low-frequency rTMS is the most common method, probably due to the fact that low-frequency rTMS is safer and has lower probability of epileptic complications [7], [20]. We therefore recorded EEG before and up to 70 min after a 15 min train of 1 Hz rTMS over the right motor cortex, in healthy subjects in the resting state and with their eyes open. The aftereffects of rTMS on the subjects' brain activity were assessed by assessing power changes of the EEG spectra and functional connectivity changes based on a weighted phase lag index (wPLI). And, the graph theory techniques were used for the analysis of functional network topologies [28], [29].

II. METHODS

A. Subjects

Twenty right-handed healthy adults (15 males and five females, average age 22.5 ± 2.36 years (mean \pm standard deviation) ranging from 20 to 28 years) were recruited for this study. No subject reported any mental or neurological diseases or related family with such a disease. The study was approved by the ethical committee of Institute of Automation, Chinese Academy of Science. All subjects gave written informed consent before participation. The purpose and procedure of the experiment were clearly explained to each subject before the EEG recordings.

B. Experimental Design

Participants sat in an armchair with their hands relaxed in front of a computer screen. The experimental procedure is visualized in Figure 1. Ten minutes of resting state EEG were recorded with the subjects having their eyes open before rTMS ("Pre"). After 5min' rest, subjects underwent one rTMS session at a frequency of 1 Hz, which lasted 15min. Then, four 10 min EEG sessions were recorded with the subjects having their eyes open, in resting state immediately after, and 20, 40, and 60 min after rTMS ("Post0", "Post20", "Post40", "Post60", respectively). All participants were told to relax as much as possible and focus on the "REST" on the screen during all experimental sessions. Also, participants were told not to think of anything specific and stay awake all the times. After each session, participants were asked to

describe: (1) whether they stayed fully awake through this session; (2) whether they experienced that their mind was no longer “black”. If the participant cannot meet any one of the criteria (they stayed fully awake; their mind was “blank”), he/she would be asked to stop this experiment and drop out of this study. To reduce the externally induced heterogeneity of the resting state condition, all participants have had a similar experimental procedure.

C. Repetitive Transcranial Magnetic Stimulation

rTMS was delivered through a circular coil connected to an S-series stimulator (YINGCHI Inc., Shenzhen, China). The coil was placed tangentially to the scalp with the handle pointing posteriorly for all stimulations. The target of stimulation was the hand area of the right motor cortex; the optimal scalp position was selected based on induced motor-evoked potentials (MEPs) in the left abductor pollicis brevis muscle (APB) for each individual. We used a robotic arm system (YINGCHI Inc., Shenzhen, China) to keep the brain target sites constant throughout and across all the stimulation sessions.

Prior to the experimental sessions, each subject's individual resting motor threshold (RMT) was defined as the stimulation intensity that elicited MEPs of more than 50 μ V in at least five out of 10 consecutive responses. During the stimulation sessions, 1 Hz rTMS was applied at 100% RMT for 15 min (900 pulses) over the right motor cortex. For low-frequency stimulation (1Hz), threshold (rather than subthreshold) stimulation (100% RMT) was used in this work as it is more reliably associated with changes to cortical excitability [8], [11]. Also, we applied 15min of rTMS based on previous literature concerning significant effects of 1 Hz rTMS [30]–[32].

D. EEG Recordings and Preprocessing

Thirty-channel EEG data were recorded with a Brainamp DC system (BrainProducts Inc., Munich, Germany) using the international 10-10 system. Figure 2 shows 30-channel EEG cap layout used in the present study. TP9 served as the reference, and the prefrontal lobe served as the ground. We set the band-pass filter at DC to 200 Hz and sampled at 5000 Hz. A 50-Hz notch filter was used during data acquisition. The skin/electrode impedance was kept below 5k Ω throughout the experiment.

During the pre-processing, the raw EEG data with a sampling frequency of 5000Hz were down-sampled to 250 Hz. The signals were referenced to the average of all electrodes using a common average reference (CAR). Afterwards, the data were band-pass filtered at 1-45 Hz. The first and last 10 s of data were discarded from the 10 min resting state EEG recording of each session. Then, the data were segmented into consecutive 2-s epochs for data rejection and analysis. Noisy data segments with apparent artifacts (high-amplitude artifactual events, eye blinks, and muscle artifacts) were detected and rejected. The subsequent spectral power and functional connectivity analysis was conducted on these 2-s data segments.

E. Estimation of Power and Functional Connectivity

The power spectra densities were computed using a fast Fourier transform (FFT) algorithm with a frequency resolution

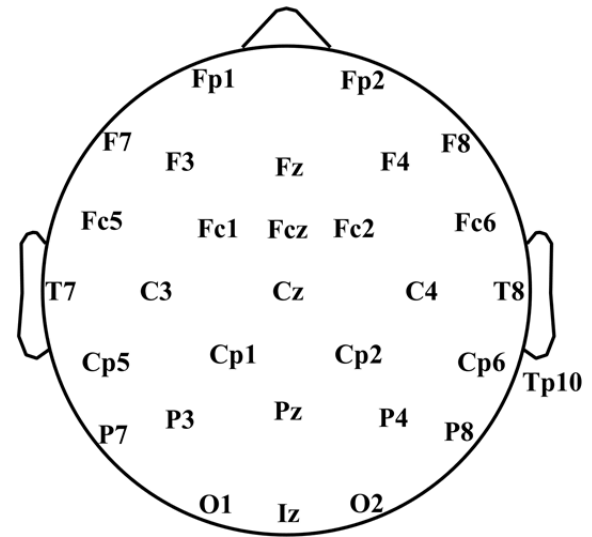


Fig. 2. 30-electrode positions.

of $1/2 \text{ s} = 0.5 \text{ Hz}$ for each 2-s segment and were then averaged across epochs. The theta, alpha, low-beta, mid-beta, and high-beta band power for each channel in each experimental session were computed as the mean power between 4 and 8 Hz, 8 and 12 Hz, 13 and 18 Hz, 18 and 24 Hz, and 24 and 30 Hz [10].

The 2-s data segment was bandpass-filtered to isolated EEG activity using a finite impulse response filter with each of the following frequency bands: theta (4-8Hz), alpha (8-12Hz), low-beta (13-18Hz), mid-beta (18-24Hz), and high-beta (24-30Hz). The wPLI was used to estimate the functional connectivity between all pairwise combinations of 30 channels independently for each 2-s filtered data segment. This is a measure of phase synchronization that is capable of minimizing effects of volume conduction by weighing each phase difference according to the magnitude of the lag [33], [34]. Given the two real-valued signals $x(t)$ and $y(t)$, their instantaneous phase difference at time point i , $\Delta\phi(t_i)$, can be obtained using the instantaneous phase of $x(t)$ and $y(t)$ based on the Hilbert transform. The wPLI was defined as

$$\text{wPLI} = \left\langle \left| \frac{|\sin \Delta\phi(t_i)|}{\sin(|\Delta\phi(t_i)|)} \right| \right\rangle \quad (1)$$

where $\langle \cdot \rangle$ denotes the average over time and $|\cdot|$ is the absolute value function. The wPLI value is between 0 and 1; it equals to 1 if $x(t)$ and $y(t)$ are maximally synchronized, and 0 if there is no synchronization between the two signals. The wPLI values between all electrode pairs were calculated and averaged, resulting in a 30*30 connectivity matrix for each segment. Then, the averaged connectivity matrix for each session was obtained by averaging the connectivity matrices of all segments from that session.

F. Partition of All Electrodes

To evaluate changes in network topologies induced by rTMS, we constructed undirected graphs for each session. In order to reduce spurious edges, we kept edges with large connection weights and deleted some edges that had small connection weights based on the sparsity threshold (S). To enable the comparison of functional connectivity networks across

experimental sessions and subjects, we retained $S\%$ of the top connections for each connectivity graph. For network analyses based on EEG, Yi *et al.* used a threshold of 0.6; Zhang *et al.* set 0.77 as the sparsity level; and 0.67 was used in Polania's study [35], [36]. Following their work, the sparsity value of the present study was set to 0.65.

In order to study changes of functional connectivity in relatively global area, functional connections were grouped along the anterior-posterior and right-left axes and divided into posterior-anterior region and left-right hemisphere [10], [20]. This was used to analyze relatively global properties compared with the local properties of the node. Also, the connections in the inter-region and inter-hemisphere can be considered as long connections in the network, while the connection in the intra-region and intra-hemisphere can be considered as short connections. Thus, this partition was also used to analyze the changes of long connections and the changes of short connections. In the anterior-posterior analysis, the EEG channels were first partitioned into anterior, central, and posterior regions. The anterior region consisted of Fp1, Fp2, F7, F3, Fz, F4, F8, Fc5, Fc1, Fcz, Fc2, and Fc6. The central region consisted of T7, C3, Cz, C4, and T8. The posterior region consisted of Cp5, Cp1, Cp2, Cp6, Tp10, P7, P3, Pz, P4, P8, O1, Iz, and O2. If two electrodes were in the anterior region, or if one of the electrodes was in the anterior region and the other was in the central region, the connection between the two was labeled an "anterior" connection. If two electrodes were in the posterior region, or if one of the electrodes was in the posterior region and the other was in the central region, the connection between the two was labeled a "posterior" connection. If one electrode was in the anterior region and the other was in the posterior region, the connection was labeled "inter-regional". Connections between two central electrodes were ignored.

To analyze within-hemisphere changes in connectivity following rTMS, these EEG channels were partitioned into the left hemispheric, the right hemispheric, and midline subsets. The left hemisphere consisted of Fp1, F7, F3, Fc5, Fc1, T7, C3, Cp5, Cp1, P7, P3, and O1. The right hemisphere consisted of Fp2, F8, F4, Fc6, T8, C4, Cp6, Cp2, P8, P4, and O2. The midline part consisted of Fz, Fcz, Cz, Pz, and Iz. If two electrodes were in the right hemispheric region, or if one of the electrodes was in the right hemispheric region and the other was in the midline region, the connection between the two electrodes was labeled a "right hemispheric" connection. If both electrodes were in the left hemispheric region, or if one electrode was in the left hemispheric region and the other was in the midline region, the connection was labeled a "left hemispheric" connection. If one electrode was in the right hemispheric region and the other was in the left hemispheric region, the connection was labeled "inter-hemispheric". Connections between two midline electrodes were ignored.

G. Graph Theory Analysis

We constructed a network based on wPLI measures, with the electrode as the node, and the wPLI values as the link weights. Then, three local properties, degree, clustering coefficient, and efficiency, were calculated to study the centrality and

information transmission ability of the nodes in the brain functional network. The degree of node i was defined as the number of edges the node i shares with other nodes. A greater degree indicates more edges and the node can thus exert greater influence on the network. The degree of node i was defined as:

$$D_i = \sum_{j \in V} w_{ij} \quad (2)$$

where V is the set of all nodes in the network, and w_{ij} represents the functional connectivity between node i and node j .

The clustering coefficient quantifies the probability that nodes connected to an index node are also connected to each other. Networks with higher clustering coefficients thus have greater local efficiency of information processing and robustness. The clustering coefficient of node i was defined as:

$$C_i = \left| \frac{2E_i}{k_i(k_i - 1)} \right| \quad (3)$$

where k_i is the number of neighboring nodes connected with node i , and $k_i(k_i - 1)/2$ denotes all possible edges among the neighbor nodes of node i . E_i is the number of the existing edges between the neighbor nodes of the node i .

The efficiency of each node reflects the efficiency of information transmission, with greater values representing the more efficient information transfer. The efficiency of node i is defined as:

$$Ef_i = \frac{1}{N(N - 1)} \sum_{h, j \in V, h \neq j} \frac{1}{d_{hj}} \quad (4)$$

where d_{hj} is the length of the shortest path between nodes h and j , which contains only neighbor nodes of node i .

H. Data Analyses

Linear mixed-effects models (LMMs) were used for the analysis of the effects of rTMS on (1) the power values of each channel, (2) the functional connectivity of each pair of channels, (3) the number of connections in the intra-region, inter-region, inter-hemisphere and inter-hemisphere, (4) the node degree of each channel, (5) the nodal clustering coefficient of each channel, and (6) the node efficiency of each channel over 5 experimental sessions. The above values in each frequency band were analyzed separately. Pairwise comparisons were embedded in LMMs to analyze the effects between Post0 and Pre, Post20 and Pre, Post40 and Pre, and Post60 and Pre. All LMMs included a random effect for each participant. Post-hoc analyses were performed using the Holm-Bonferroni correction for four comparisons. Statistical significance was set to 0.05. All results are presented as mean \pm standard deviation (SD). All analyses were performed using Matlab software (Mathworks Inc., MA, US).

III. RESULT

A. Resting State Power

The effects of rTMS on the power of low-beta, mid-beta, and high-beta bands in each channel were not significant (see Figure S1 in the Supplementary Material). The resting power of the three beta frequency bands remained stationary throughout the entire course of the experiment.

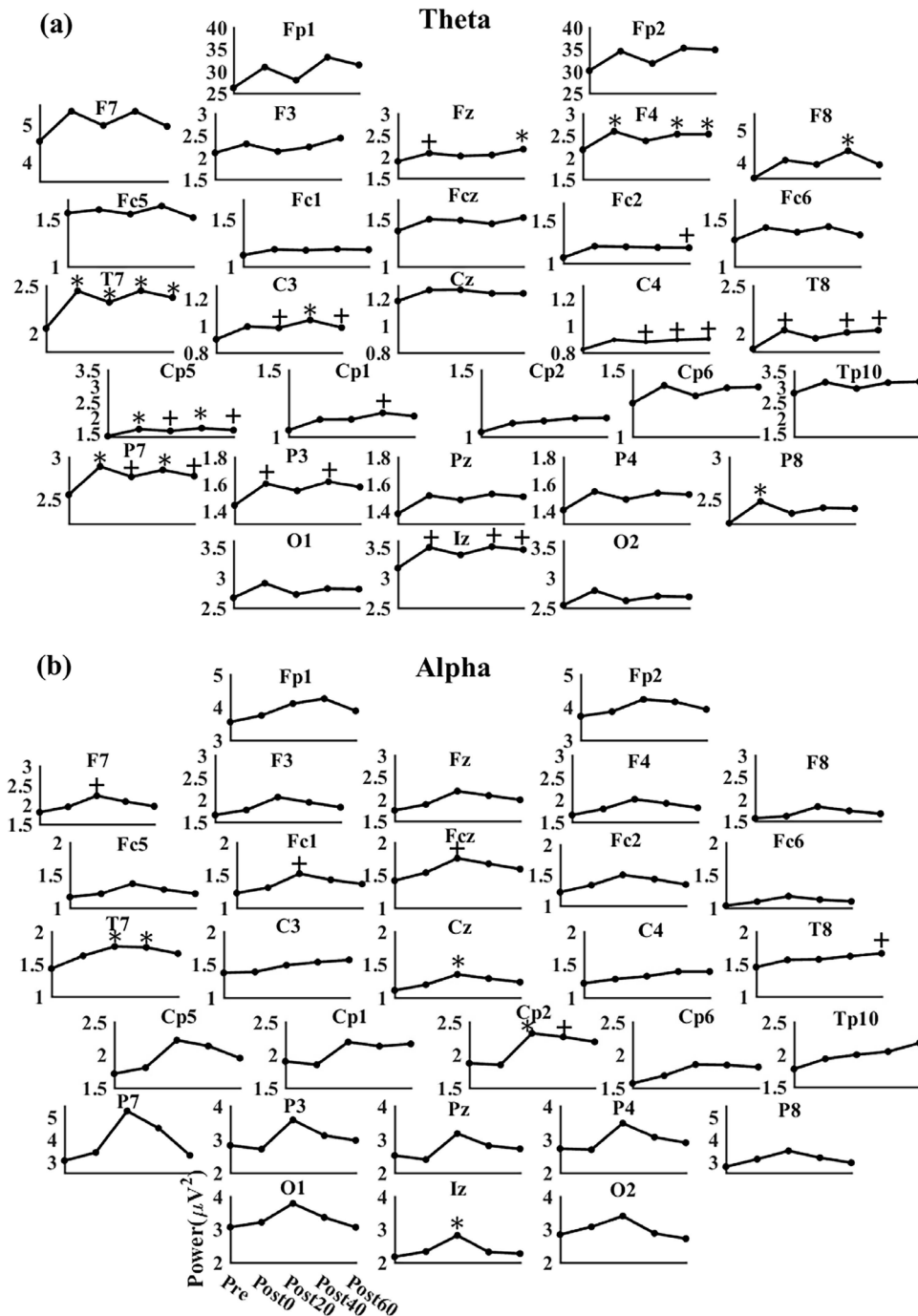


Fig. 3. The power (mean \pm SD) for each electrode over the five sessions before and after rTMS in theta (a) and alpha frequency band (b). * denotes a significant difference between the present session and the session before rTMS (Pre) ($p < 0.05$), + denotes a difference that tended to be significant between the present session and the session before rTMS (Pre) ($p < 0.1$).

Figure 3(a) shows the power changes in each channel in the theta band. Significant increases in theta-band power at CP5 were observed immediately after rTMS ($p < 0.05$) and in Post40 ($p < 0.05$), and power at both Post20 and Post60 tended to be higher than before rTMS ($p < 0.1$). Similarly, for P7, power at both Post0 and Post40 was significantly higher than power before rTMS ($p < 0.05$), and power at both Post20 and Post60 tended to be higher than before rTMS ($p < 0.1$). For T7, significant increases in theta-band power were observed in all four sessions after rTMS ($p < 0.05$). For F4, except

at Post20, power was significantly higher after than before rTMS ($p < 0.05$), and power at Post20 tended to be higher than power before rTMS ($p = 0.11$). For Fz, power at Post60 was significantly higher than power before rTMS ($p < 0.05$), and power at Post20 tended to be higher than before rTMS ($p < 0.1$). For C3, power at Post40 was significantly higher than power at Pre, and power values at Post0, Post20, and Post60 tended to be higher than power before rTMS (Post0: $p = 0.11$, Post20: $p < 0.1$, Post60: $p < 0.1$). For C4, power values at Post20, Post40 and Post60 tended to be higher than power

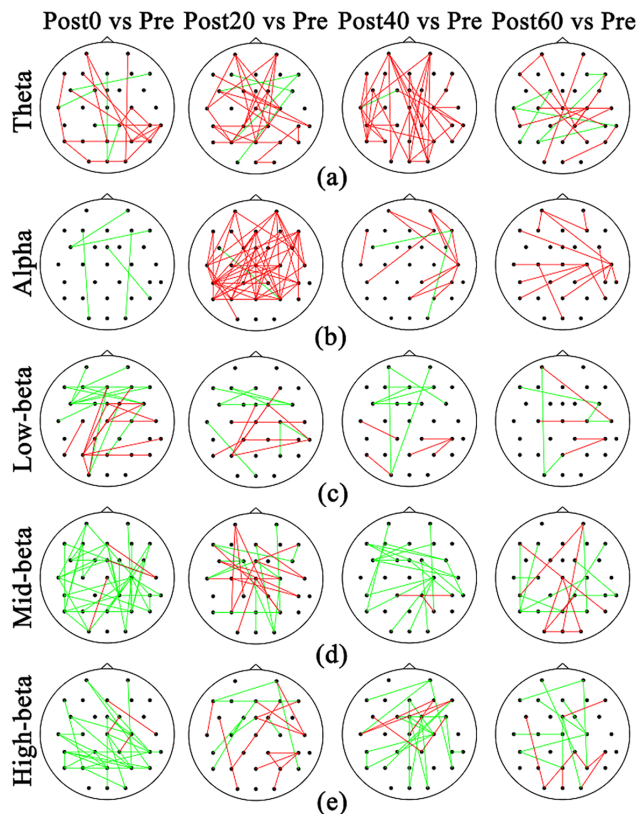


Fig. 4. Functional connectivity changes after rTMS (compared with Pre) with significant increases (red) or decreases (green) across subjects in theta (a), alpha (b), low-beta (c), mid-beta (d), or high-beta frequency band (e).

before rTMS (Post20: $p < 0.1$, Post40: $p < 0.1$, Post60: $p < 0.1$). Figure 3(b) shows the power changes in each channel in the alpha band. For Cp2, an increase in power occurred at 20min after rTMS but not immediately after rTMS ($p < 0.05$), and power at 40min after rTMS tended to be higher than power before rTMS ($p < 0.1$). For Cz and Iz, the analysis revealed an increase in power at 20min after rTMS, compared to Pre ($p < 0.05$). For Fc1, Fcz and F7, power at 20 min after rTMS tended to be higher than power before rTMS ($p < 0.1$).

B. Functional Connectivity

Figure 4 shows the connections with significant changes in functional connectivity after rTMS in each frequency band. In the alpha band, Figure 4(b) shows a decrease in connectivity immediately after rTMS, and a widespread increase in functional connectivity at Post20. There is also an increase in functional connectivity at Post40 and Post60. In the theta band, there appears to be a decrease in inter-hemispheric connections, with a concomitant increase in intra-regional or short-range connections at Post0, Post20, and Post60. There is a widespread increase in functional connectivity in Post40. In the low-beta, mid-beta, and high-beta band, there is a widespread decrease in functional connectivity immediately after rTMS.

For the chosen sparsity level of 0.65, the observed changes in the numbers of intra-hemispheric, inter-hemispheric, intra-regional, and inter-regional connections in the alpha band induced by rTMS are shown in Figure 5. There were no

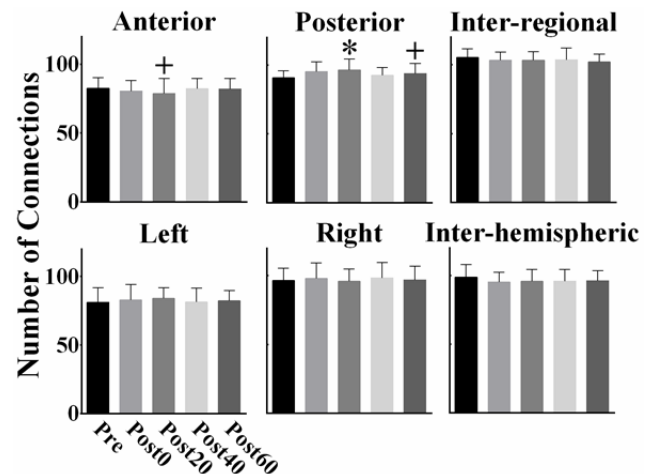


Fig. 5. The changes in the number of connections induced by rTMS in the anterior, the posterior, the inter-regional, the left hemispheric, the right hemispheric, and the inter-hemispheric regions in the alpha band. * denotes a significant difference between the present session and the session before rTMS (Pre) ($p < 0.05$), + denotes a difference that tended to be significant between the present session and the session before rTMS (Pre) ($p < 0.1$).

significant differences in the numbers of intra-hemispheric, inter-hemispheric, inter-regional connections between the sessions before and each session after rTMS. In the posterior region, there was a significant increase in the number of connections at 20min after rTMS ($p < 0.05$), and then, a weak increase at 60min after rTMS ($p < 0.1$). In the anterior region, in contrast, there was a weak decrease in the number of connections at 20min after rTMS ($p < 0.1$). In the theta band, and the three beta bands, the changes in the numbers of intra-hemispheric inter-hemispheric, intra-regional and inter-regional connections induced by rTMS were not statistically significant (see Figure S2 in the Supplementary Material).

C. Changes in Network Characteristics

The significant changes in the three nodal characteristics of the networks are shown in Figures 6-8. There were no significant changes in node degree in the low-beta band. In the theta band, for Cp5, P7, and O2, an increase in node degree was found after rTMS, which reached significance at Post40 ($p < 0.05$) (Figure 6(a)). In the alpha band (Figure 6(b)), for Cp5, a significant increase in node degree was found at 20min after rTMS ($p < 0.05$), and the degree of P3 and P4 tended to be higher at Post20 than at Pre ($p < 0.1$). In the mid-beta band (Figure 6(c)), for Fc2, a significant decrease in node degree was found at 40min after rTMS ($p < 0.05$). For Fz, there was a decrease in node degree at 60min after rTMS ($p < 0.1$). Also, and the degree of P8 at Post20 tended to be higher than that at Pre ($p < 0.1$). In the high-beta band (Figure 6(d)), for P3, P7, and P8, there was a significant decrease in node degree immediately after rTMS ($p < 0.05$).

As for the clustering coefficient, there were no significant changes in the low-beta, mid-beta and high-beta band. As shown in Figure 7(a), in the theta band, for Fc6, F8, F4 and T8, a significant decrease in the clustering coefficient was found immediately after rTMS ($p < 0.05$). For Cp2, significant decreases in the clustering coefficient were found immediately after rTMS and at 40min after rTMS ($p < 0.05$). For Pz,

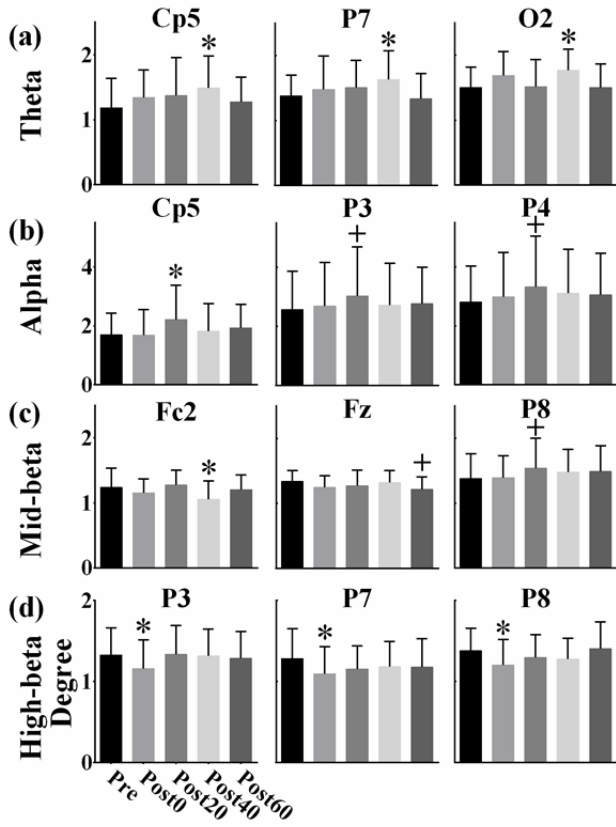


Fig. 6. The changes of node degree in Cp5, P7, and O2 electrodes in the theta frequency band (a), in Cp5, P3, and P4 electrodes in the alpha band (b), in Fc2, Fz, and P8 electrodes in the mid-beta band (c), and P3, P7 and P8 electrodes in the high-beta band (d). * denotes a significant difference between the present session and the session before rTMS (Pre) ($p < 0.05$), + denotes a difference that tended to be significant between the present session and the session before rTMS (Pre) ($p < 0.1$).

there were significant decreases in the clustering coefficient at Post0, Post40, and Post60 ($p < 0.05$). For C3, F7 and O1, the clustering coefficient tended to be lower immediately after rTMS ($p < 0.1$). In the alpha band (Figure 7(b)), for Cp6 and O1, a significant decrease in the clustering coefficient was found in Post60 immediately after rTMS ($p < 0.05$). For Cp5, the clustering coefficients at Post40 and Post60 tended to be lower than that at Pre ($p < 0.1$). There was a decreasing trend in the clustering coefficient after rTMS.

Regarding the node efficiency, there were no significant changes in any node in the low-beta band. In the theta band (Figure 8(a)), for O2, a significant increase in nodal efficiency was found at 40min after rTMS ($p < 0.05$). The efficiency of Fc2 tended to be higher at Post20 and at Post40 ($p < 0.1$). For P7, the efficiency at Post40 tended to be higher than that at Pre ($p < 0.1$). In the alpha band (Figure 8(b)), the efficiency of Cp5 at Post20 tended to be higher than that at Pre. Also, the efficiency of T8 tended to be higher at Post60 ($p < 0.1$). In the mid-beta band (Figure 8(c)), for Pz, there were a significant decrease in the node efficiency immediately after rTMS ($p < 0.05$), and then a recovery at 20min after rTMS. In the high-beta band (Figure 8(d)), For P3 and P7, there were a significant decrease in efficiency immediately after rTMS ($p < 0.05$), and then a recovery at 20min after rTMS.

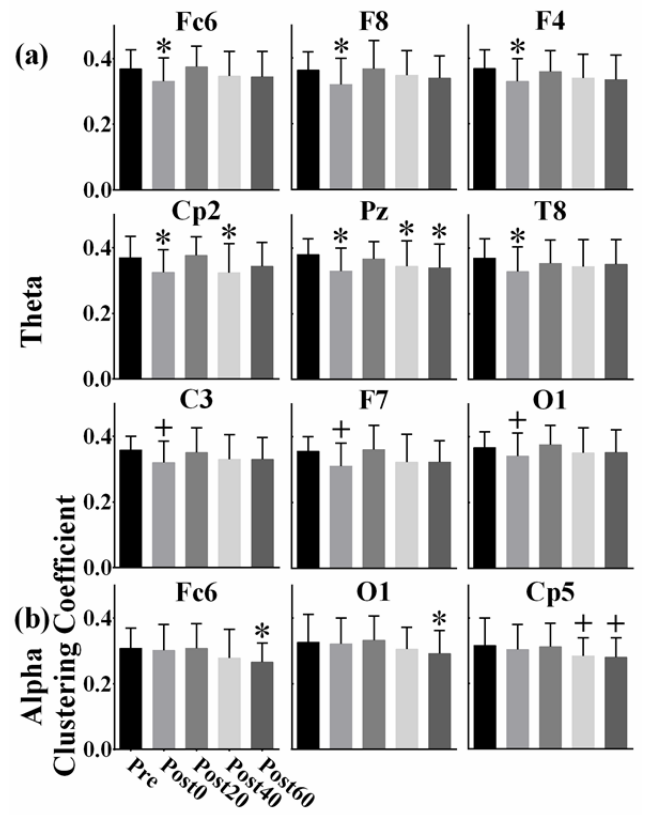


Fig. 7. The changes of clustering coefficient in Fc6, F8, F4, Cp2, Pz, T8, C3, F7, and O1 electrodes in the theta frequency band (a), and in Fc6, O1 and Cp5 in the alpha frequency band (b). * denotes a significant difference between the present session and the session before rTMS (Pre) ($p < 0.05$), + denotes a difference that tended to be significant between the present session and the session before rTMS (Pre) ($p < 0.1$).

The changes of the nodal characteristics of the networks in each channel are shown in Figures S3-S5 in the Supplementary Material.

IV. DISCUSSION

In the present study, we investigated the effects of low-frequency rTMS over the right motor cortex on neural oscillations and functional connectivity using EEG signals up to 70min after rTMS. We found that 1-Hz rTMS induced a long effect on alpha-band power, beta-band power, the clustering coefficient, and the node degree. Some of the aftereffects changed dynamically rather than linearly. Moreover, our results demonstrate the inhibitory effect of 1-Hz rTMS near the site of stimulation. In addition, low-frequency rTMS produced alterations in power and nodal degree in non-stimulated regions.

In line with previous studies [27], [37], we found that the alpha-band and beta-band power at C3 and C4 were unaffected by low-frequency rTMS. Significant changes in alpha-band oscillations were found in the frontoparietal brain area (F7, Fc1, Fcz, Cz and Cp2), which showed a delayed increase in power values. A previous study found that the reduction of MEP amplitude was accompanied by a significant increase of 11–13 Hz oscillations over the sensorimotor areas during an inhibitory motor paradigm [38]. Therefore, the increase in alpha-band power implies that 1Hz rTMS induced inhibition of

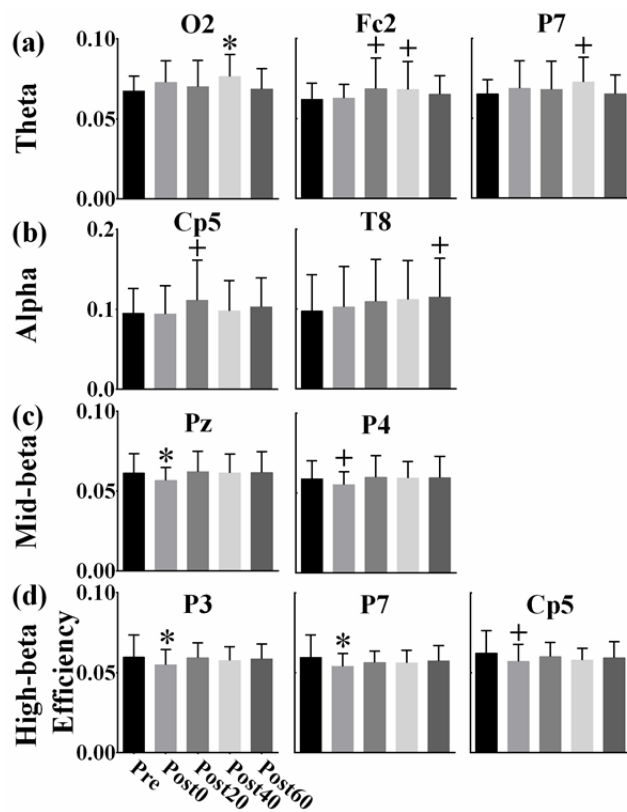


Fig. 8. The changes of node efficiency in O2, Fc2, and P7 electrodes in the theta frequency band (a), in Cp5 and T8 in the alpha band (b), in Pz and P4 electrodes in the mid-beta frequency band (c), and in P3, P7 and Cp5 in the high-beta frequency band (d). * denotes a significant difference between the present session and the session before rTMS (Pre) ($p < 0.05$), + denotes a difference that tended to be significant between the present session and the session before rTMS (Pre) ($p < 0.1$).

the brain. At the same time, low-frequency rTMS induced significant immediate increases in the power values of theta-band oscillations in the centroparietal brain areas contralateral to the stimulation site and in the frontal brain area ipsilateral to the stimulation site. Even though we tested resting state EEG recordings up to 70min after rTMS, but did not find a recovery during the last experimental session. These observations indicate that low-frequency rTMS produces long-lasting alterations in the power values of theta and alpha frequency bands in non-stimulated regions rather than in the stimulated local region under the TMS coil. In addition, beta-band power at each electrode remained stationary throughout the entire course, which indicated beta-band oscillation in the resting state was not significantly influenced by rTMS. Beta EEG are present over the frontal regions when a person is alert/attentive and thinking actively [39]. In this present study, the resting state EEG was recorded and studied when the subjects were told to relax as much as possible and told not to think anything specific and stay awake all the times. Thus, either the resting state before rTMS or the resting state after rTMS, participants were not alert/attentive and thinking actively. Moreover, low-frequency rTMS was applied over the motor cortex, which usually influences the motor functions of the brain rather than the cognitive function of the brain. Thus, low-frequency rTMS over the motor cortex may not produce the changes in alert/attentive or thinking state in the healthy subjects.

Therefore, rTMS induced less significant changes in beta-band power.

Besides analyzing changes in power induced by low-frequency rTMS, we also evaluated changes in functional connectivity, to investigate the aftereffects of rTMS based on a comparison between the session before rTMS and the four sessions after rTMS. The functional connectivity pattern revealed frequency-specific and region-specific changes. In our study, there were decreases in functional connectivity immediately after rTMS in the alpha band, which is consistent with the result of one previous study [10]. However, a widespread increase was observed in 20min after rTMS, and, a recovery after 40min. This suggests that the changes in functional connectivity in the alpha band may be not linear. In addition, there was also a regional specificity in the pattern of functional connectivity changes, with significant changes noted in the anterior and posterior connections in the alpha band. The big change in numbers of intra-regional connections was found in 30min after rTMS, compared with connections before rTMS. This indicates that the intra-regional connectivity is modulated, in line with anatomical data demonstrating greater structural connectivity between adjacent rather than distant cortical regions [40], [41].

We also calculated and compared three node properties, to study the aftereffects of rTMS. The clustering coefficient quantifies the extent to which the nearest neighbors of a given node are connected to each other, and thereby represents a measure of the extent of local connectivity [10], [42]. A large clustering coefficient represents a high efficiency of local information procession. In the alpha band, we observed a decrease in the local efficiency of information processing in the frontocentral area ipsilateral to the stimulation at 60min after rTMS, as indicated by the decrease in the clustering coefficient of Fc6. Also, in the theta band, the efficiency of local information procession was weakened induced by rTMS in right frontoparietal brain area ipsilateral to stimulation. Our results proved the inhibitory effect of 1-Hz rTMS near the site. Notably, we found that the changes in clustering coefficients after rTMS were not linear. In the theta band, the clustering coefficient decreased immediately after rTMS and recovered in 20min after rTMS, followed by another decrease without a recovery. In the alpha band, the clustering coefficient of Fc6 decreased at 60min after rTMS. This shows that low-frequency rTMS has a long-lasting effect on clustering coefficients, but that this effect is not steady. It is thus necessary to measure over multiple sessions to study dynamic changes in brain activity after rTMS. On the other hand, the degree of one node represents the number of other nodes it is connected to. The greater the degree of a node, the more important it may be in the brain network [43]. In the alpha and theta band, the importance of the non-stimulated motor area thus increased, as indicated by the increase in the node degree of Cp5 after rTMS. This suggests that low-frequency rTMS influenced the non-stimulated motor area. Similarly, in the mid-beta band, the importance of the frontocentral area ipsilateral to the stimulation site decreased, as indicated by the decrease in node degree of Fc2. Therefore, these findings provide direct evidence for the

interhemispheric competition. Based on the concept of interhemispheric competition, low-frequency rTMS is increasingly used to induce inhibitory interactions to promote motor recovery in stroke rehabilitation. Although many previous studies have demonstrated the inhibition of the motor cortex induced by 1-Hz rTMS through the behavioral effects on the ipsilateral hand [44]–[46], to the best of our knowledge, this study is the first to corroborate this inhibitory effect of 1-Hz rTMS via nodal properties of EEG networks, which provides more direct measurements. In addition, node efficiency indicates how well a specific region is integrated within the network via its shortest paths. A large efficiency value thus represents a high efficiency of information integration and distribution. In the alpha band, the node efficiency of the information integration and distribution in the centroparietal brain areas increased at 20 min after rTMS, as indicated by the weak increase in the node efficiency of Cp5 after rTMS. At the same time, in the mid-beta and high-beta band, the efficiency in the parietal area decreased immediately after rTMS, and followed with a recovery. These changes in the beta band induced by rTMS occurred immediately after rTMS, and kept in a short time (<20min).

Our study has several limitations. Firstly, we did not include a sham group. Future studies should thus consider to include a group of control subjects. Secondly, future studies should combine a network analysis technique such as the one described here with behavioral data before and after rTMS to assess and understand the aftereffect of rTMS in more detail.

V. CONCLUSION

In summary, our findings suggest that low-frequency rTMS induces long-lasting changes in power and functional connectivity. The results of our network analysis provide direct evidence for the inhibitory effect of low-frequency rTMS near the site of stimulation. The methods used in this study might be a promising approach to study dynamic changes in brain activity after rTMS, and the findings presented here provide useful directions for future research on the effects of low-frequency rTMS in patients with stroke.

ACKNOWLEDGMENT

The authors would like to thank Prof. Y. Zhang and Prof. T. Jiang from the Institute of Automation, Chinese Academy of Sciences, Beijing, China, for their invaluable help in doing this experiment.

REFERENCES

- [1] A. T. Barker, R. Jalinous, and I. L. Freeston, "Non-invasive magnetic stimulation of human motor cortex," *Lancet*, vol. 325, no. 8437, pp. 1106–1107, May 1985.
- [2] A. Cowey and V. Walsh, "Tickling the brain: Studying visual sensation, perception and cognition by transcranial magnetic stimulation," *Prog. Brain Res.*, vol. 134, pp. 9–17, Jan. 2001.
- [3] Y. Terao and Y. Ugawa, "Studying higher cerebral functions by transcranial magnetic stimulation," *Suppl. Clin. Neurophysiol.*, vol. 59, pp. 9–17, Jan. 2006.
- [4] A. Pascual-Leone, D. Bartres-Faz, and J. P. Keenan, "Transcranial magnetic stimulation: Studying the brain-behaviour relationship by induction of 'virtual lesions,'" *Philos. Trans. Roy. Soc. London. B, Biol. Sci.*, vol. 354, pp. 1229–1238, Jul. 1999.
- [5] R. Chen *et al.*, "Depression of motor cortex excitability by low-frequency transcranial magnetic stimulation," *Neurology*, vol. 48, no. 5, pp. 1398–1403, May 1997.
- [6] S. M. Brodie, S. Meehan, M. R. Borich, and L. A. Boyd, "5 Hz repetitive transcranial magnetic stimulation over the ipsilesional sensory cortex enhances motor learning after stroke," *Frontiers Hum. Neurosci.*, vol. 8, p. 143, Mar. 2014, doi: [10.3389/fnhum.2014.00143](https://doi.org/10.3389/fnhum.2014.00143).
- [7] L. Sebastianelli *et al.*, "Low-frequency rTMS of the unaffected hemisphere in stroke patients: A systematic review," *Acta Neurologica Scandinavica*, vol. 136, no. 6, pp. 585–605, Dec. 2017.
- [8] P. Fitzgerald, S. Fountain, and Z. Daskalakis, "A comprehensive review of the effects of rTMS on motor cortical excitability and inhibition," *Clin. Neurophysiol.*, vol. 117, no. 12, pp. 2584–2596, Dec. 2006.
- [9] C. Baeken, D. L. Schrijvers, B. G. C. Sabbe, M. A. Vanderhasselt, and R. De Raedt, "Impact of one HF-rTMS session on fine motor function in right-handed healthy female subjects: A comparison of stimulation over the left versus the right dorsolateral prefrontal cortex," *Neuropsychobiology*, vol. 65, no. 2, pp. 96–102, 2012.
- [10] M. M. Shafi, M. Brandon Westover, L. Oberman, S. S. Cash, and A. Pascual-Leone, "Modulation of EEG functional connectivity networks in subjects undergoing repetitive transcranial magnetic stimulation," *Brain Topography*, vol. 27, no. 1, pp. 172–191, Jan. 2014.
- [11] G. Thut and A. Pascual-Leone, "A review of combined TMS-EEG studies to characterize lasting effects of repetitive TMS and assess their usefulness in cognitive and clinical neuroscience," *Brain Topography*, vol. 22, no. 4, pp. 219–232, Jan. 2010.
- [12] F. Maeda, J. P. Keenan, J. M. Tormos, H. Topka, and A. Pascual-Leone, "Modulation of corticospinal excitability by repetitive transcranial magnetic stimulation," *Clin. Neurophysiol.*, vol. 111, no. 5, pp. 800–805, May 2000.
- [13] A. May *et al.*, "Structural brain alterations following 5 days of intervention: Dynamic aspects of neuroplasticity," *Cerebral Cortex*, vol. 17, no. 1, pp. 205–210, Jan. 2007.
- [14] A. Avenanti, M. Coccia, E. Ladavas, L. Provinciali, and M. G. Ceravolo, "Low-frequency rTMS promotes use-dependent motor plasticity in chronic stroke: A randomized trial," *Neurology*, vol. 78, no. 4, pp. 256–264, Jan. 2012.
- [15] M. N. McDonnell and C. M. Stinear, "TMS measures of motor cortex function after stroke: A meta-analysis," *Brain Stimulation*, vol. 10, no. 4, pp. 721–734, Jul. 2017.
- [16] B. O. Adeyemo, M. Simis, D. D. Macea, and F. Fregni, "Systematic review of parameters of stimulation, clinical trial design characteristics, and motor outcomes in noninvasive brain stimulation in stroke," *Front Psychiatry*, vol. 3, no. 8, doi: [10.3389/fpsy.2012.00088.2012](https://doi.org/10.3389/fpsy.2012.00088.2012).
- [17] N. Kubis, "Non-invasive brain stimulation to enhance post-stroke recovery," *Front Neural Circuits*, vol. 10, p. 56, Jul. 2016, doi: [10.3389/fncir.2016.00056](https://doi.org/10.3389/fncir.2016.00056).
- [18] L. Ding, G. Shou, H. Yuan, D. Urbano, and Y.-H. Cha, "Lasting modulation effects of rTMS on neural activity and connectivity as revealed by resting-state EEG," *IEEE Trans. Biomed. Eng.*, vol. 61, no. 7, pp. 2070–2080, Jul. 2014.
- [19] S. W. Chung, N. C. Rogasch, K. E. Hoy, and P. B. Fitzgerald, "Measuring brain stimulation induced changes in cortical properties using TMS-EEG," *Brain Stimulation*, vol. 8, no. 6, pp. 1010–1020, Nov. 2015.
- [20] J. N. Jin, X. Wang, Y. Li, F. Jin, Z. P. Liu, and T. Yin, "The effects of rTMS combined with motor training on functional connectivity in alpha frequency band," *Frontiers Behav. Neurosci.*, vol. 11, p. 234, Nov. 2017, doi: [10.3389/fnbeh.2017.00234](https://doi.org/10.3389/fnbeh.2017.00234).
- [21] G. Leodori, N. Thiruganasambandam, H. Conn, T. Popa, A. Berardelli, and M. Hallett, "Intracortical inhibition and surround inhibition in the motor cortex: A TMS-EEG study," *Frontiers Neurosci.*, vol. 13, p. 612, Jun. 2019, doi: [10.3389/fnins.2019.00612](https://doi.org/10.3389/fnins.2019.00612).
- [22] P. Canali *et al.*, "Changes of cortical excitability as markers of antidepressant response in bipolar depression: Preliminary data obtained by combining transcranial magnetic stimulation (TMS) and electroencephalography (EEG)," *Bipolar Disorders*, vol. 16, no. 8, pp. 809–819, Dec. 2014.
- [23] G. Thut and C. Miniussi, "New insights into rhythmic brain activity from TMS-EEG studies," *Trends Cogn. Sci.*, vol. 13, no. 4, pp. 182–189, Apr. 2009.
- [24] I. Griskova, E. F. Pavone, A. Fiaschi, and P. Manganotti, "The effects of 10 Hz repetitive transcranial magnetic stimulation on resting EEG power spectrum in healthy subjects," *Neurosci. Lett.*, vol. 419, no. 2, pp. 162–167, 2007.
- [25] G. Fuggetta, E. F. Pavone, A. Fiaschi, and P. Manganotti, "Acute modulation of cortical oscillatory activities during short trains of high-frequency repetitive transcranial magnetic stimulation of the human motor cortex: A combined EEG and TMS study," *Hum. Brain Mapping*, vol. 29, no. 1, pp. 1–13, Jan. 2008.

- [26] S. Li, J. N. Jin, X. Wang, H. Z. Qi, Z. P. Liu, and T. Yin, "Theta and alpha oscillations during the retention period of working memory by rTMS stimulating the parietal lobe," *Frontiers Behav. Neurosci.*, vol. 11, no. 170, doi: [10.3389/fnbeh.2017.00170.2017](https://doi.org/10.3389/fnbeh.2017.00170.2017).
- [27] D. Desideri, C. Zrenner, P. C. Gordon, U. Ziemann, and P. Belardinelli, "Nil effects of μ -rhythm phase-dependent burst-rTMS on cortical excitability in humans: A resting-state EEG and TMS-EEG study," *PLoS ONE*, vol. 13, no. 12, Dec. 2018, Art. no. e0208747, doi: [10.1371/journal.pone.0208747](https://doi.org/10.1371/journal.pone.0208747).
- [28] C. J. Stam and J. C. Reijneveld, "Graph theoretical analysis of complex networks in the brain," *Nonlinear Biomed. Phys.*, vol. 1, no. 1, p. 3, Dec. 2007, doi: [10.1186/1753-4631-1-3](https://doi.org/10.1186/1753-4631-1-3).
- [29] E. Bullmore and O. Sporns, "Complex brain networks: Graph theoretical analysis of structural and functional systems," *Nature Rev. Neurosci.*, vol. 10, no. 3, pp. 186–198, Mar. 2009.
- [30] E. M. Khedr, M. R. Abdel-Fadeil, A. Farghali, and M. Qaid, "Role of 1 and 3 Hz repetitive transcranial magnetic stimulation on motor function recovery after acute ischaemic stroke," *Eur. J. Neurol.*, vol. 16, no. 12, pp. 1323–1330, Dec. 2009.
- [31] P. G. Enticott, N. J. Rinehart, B. J. Tonge, J. L. Bradshaw, and P. B. Fitzgerald, "Repetitive transcranial magnetic stimulation (rTMS) improves movement-related cortical potentials in autism spectrum disorders," *Brain Stimulation*, vol. 5, no. 1, pp. 30–37, Jan. 2012.
- [32] W.-H. Chen *et al.*, "Low-frequency rTMS over lateral premotor cortex induces lasting changes in regional activation and functional coupling of cortical motor areas," *Clin. Neurophysiol.*, vol. 114, no. 9, pp. 1628–1637, Sep. 2003.
- [33] E. Ortiz, K. Stingl, J. Münßinger, C. Braun, H. Preissl, and P. Belardinelli, "Weighted phase lag index and graph analysis: Preliminary investigation of functional connectivity during resting state in children," *Comput. Math. Methods Med.*, vol. 2012, pp. 1–8, Sep. 2012, doi: [10.1155/2012/186353](https://doi.org/10.1155/2012/186353).
- [34] M. Vinck, R. Oostenveld, M. van Wingerden, F. Battaglia, and C. M. A. Pennartz, "An improved index of phase-synchronization for electrophysiological data in the presence of volume-conduction, noise and sample-size bias," *NeuroImage*, vol. 55, no. 4, pp. 1548–1565, Apr. 2011.
- [35] W. Yi *et al.*, "Evaluation of EEG oscillatory patterns and cognitive process during simple and compound limb motor imagery," *PLoS ONE*, vol. 9, no. 12, Dec. 2014, Art. no. e114853, doi: [10.1371/journal.pone.0114853](https://doi.org/10.1371/journal.pone.0114853).
- [36] Y. Zhang, P. Xu, D. Guo, and D. Yao, "Prediction of SSVEP-based BCI performance by the resting-state EEG network," *J. Neural Eng.*, vol. 10, no. 6, 2013, Art. no. 066017, doi: [10.1088/1741-2560/10/6/066017](https://doi.org/10.1088/1741-2560/10/6/066017).
- [37] S. M. McAllister, J. C. Rothwell, and M. C. Ridding, "Cortical oscillatory activity and the induction of plasticity in the human motor cortex," *Eur. J. Neurosci.*, vol. 33, no. 10, pp. 1916–1924, May 2011.
- [38] F. Hummel, F. Andres, E. Altenmüller, J. Dichgans, and C. Gerloff, "Inhibitory control of acquired motor programmes in the human brain," *Brain*, vol. 125, no. 2, pp. 404–420, Feb. 2002.
- [39] C. Kirstein, "Sleeping and dreaming," in *xPharm: The Comprehensive Pharmacology Reference*, vol. 446, 2007, pp. 1–4.
- [40] P. Hagmann *et al.*, "Mapping the structural core of human cerebral cortex," *PLoS Biol.*, vol. 6, no. 7, Jul. 2008, Art. no. e159, doi: [10.1371/journal.pbio.0060159](https://doi.org/10.1371/journal.pbio.0060159).
- [41] J. D. Lewis, R. J. Theilmann, M. I. Sereno, and J. Townsend, "The relation between connection length and degree of connectivity in young adults: A DTI analysis," *Cerebral Cortex*, vol. 19, no. 3, pp. 554–562, Mar. 2009.
- [42] S.-W. Xue, Y.-Y. Tang, R. Tang, and M. I. Posner, "Short-term meditation induces changes in brain resting EEG theta networks," *Brain Cognition*, vol. 87, pp. 1–6, Jun. 2014.
- [43] J. Liu *et al.*, "Complex brain network analysis and its applications to brain disorders: A survey," *Complexity*, vol. 2017, pp. 1–27, Oct. 2017, doi: [10.1155/2017/8362741](https://doi.org/10.1155/2017/8362741).
- [44] M. Kobayashi, S. Hutchinson, H. Theoret, G. Schlaug, and A. Pascual-Leone, "Repetitive TMS of the motor cortex improves ipsilateral sequential simple finger movements," *Neurology*, vol. 62, no. 1, pp. 91–98, Jan. 2004.
- [45] M. Dafotakis, C. Grefkes, L. Wang, G. R. Fink, and D. A. Nowak, "The effects of 1 Hz rTMS over the hand area of M1 on movement kinematics of the ipsilateral hand," *J. Neural Transmiss.*, vol. 115, no. 9, pp. 1269–1274, Sep. 2008.
- [46] D. A. Nowak, C. Grefkes, M. Ameli, and G. R. Fink, "Interhemispheric competition after stroke: Brain stimulation to enhance recovery of function of the affected hand," *Neurorehabilitation Neural Repair*, vol. 23, no. 7, pp. 641–656, Sep. 2009.